Arch. Min. Sci. **67** (2022), 1, 3-24

Electronic version (in color) of this paper is available: http://mining.archives.pl

DOI: https://doi.org/10.24425/ams.2022.140699

TOMASZ JANOSZEK[1], JERZY KRAWCZYK[2]

METHODOLOGY DEVELOPMENT AND INITIAL RESULTS OF CFD SIMULATIONS OF METHANE DISTRIBUTION IN THE WORKING OF A LONGWALL VENTILATED IN A SHORT "Y" MANNER

The mining in seams with a high methane content by means of a longwall system, under conditions of high extraction concentration, results in exceeding methane concentrations allowed by the regulations at workings of the longwall environment, with the effect of mining machines' standstill periods. The paper is a part of a study supporting the development of a system for shearing cutting speed control at the longwall, which should substantially reduce the production standstills due to exceeded limits and switching off the supply of electric equipment. Such a control system may be appropriate for longwalls ventilated using "Y" and "short Y" methods. Efficient Computer simulations of the 3D airflow and methane propagation may assist the design and initial evaluation of the control system performance. First chapters present studies that are necessary for a proper formulation of the properties of the longwall model. Synthetic analysis of production during the period of longwall operation allowed one to choose the input assumptions to carry out ventilation-methane computations in a CFD numerical model of longwall Z-11. This study is followed by a description of the model that is used for a case study, considering three variants of the shearer position. Finally, initial simulation results and directions of further studies are discussed.

Keywords: modelling; methane; CFD; underground mining; natural hazards; shearer

1. Introduction

Hard coal seams frequently contain methane. In underground mines, the release of this gas from coal seams and other geological strata may result in the origination of explosive mixtures in mine workings. So the underground coal mining must be carried out in a way reducing this

[1] CENTRAL MINING INSTITUTE (GIG), 1 GWARKÓW SQ., 40-166 KATOWICE, POLAND
[2] STRATA MECHANICS RESEARCH INSTITUTE, POLISH ACADEMY OF SCIENCE, 27 REYMONTA STR., 30-059 KRAKÓW, POLAND

* Corresponding author: tjanoszek@gig.eu

hazard by moving away from dangerous accumulations of this gas in the goaf from the working equipment and by the effective detection of potentially explosive methane and air mixtures via monitoring of the mine atmosphere condition [1]. In particular, this applies to a widely used method of underground mining by the means of longwalls. In this method, the source of methane is not only the process of cutting itself but also the goaf left after mining and unstressed rock layers in the longwall surroundings [2-4]. The release of methane from the goaf to the longwall depends mainly on the adopted method of ventilation, which shapes the way of this gas inflow to the workings [5].

In Polish hard coal mines approx. 70% of all mined longwalls are ventilated using the so-called "U" method on the coal solid, where the supply and return air gateroads are adjacent to the unmined coal panel. However, from the methane hazard point of view, this is the most unfavourable method of ventilation. It creates conditions for migration of dangerous methane concentration from the goaf to the longwall face or/and to the area of longwall crossing with a roadway (Fig. 1). Despite that, in numerous cases, the forecasts of endogenous fire hazards in the longwall goaf force the choice of such method of its ventilation. In the cases of high absolute methane-bearing capacity, at the simultaneous hazard of an endogenous fire, an alternative way of longwall ventilation utilising the "Y" or "short Y" method.

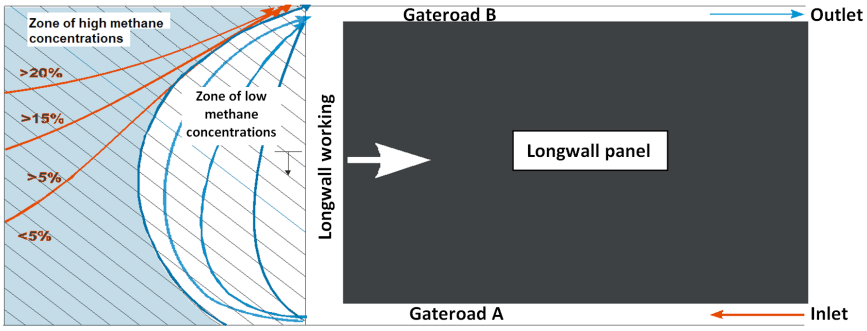

Fig. 1. Tendency of methane content distribution in the goaf of longwall ventilated by means of the "U" method

The disadvantage of U-system ventilation, shown in Figure 2, is the increase in methane hazard at the outlet of the longwall working, the necessity to use auxiliary ventilation equipment, and the difficulty in obtaining high methane drainage efficiency. The advantage of this system is the possibility to identify changes in the coal bed methane-bearing capacity, limited airflow through the goafs and limited fire hazard in goafs [1,4].

The „short Y" ventilation method, presented in Fig. 2, requires driving two parallel air roadways, one of which delivers a flow of intake air to the air outflow from the longwall, and then the return air from the area of mining is taken by this roadway and a cross-cut connecting with the air roadway. The use of the „short Y" ventilation method considerably improves the work safety conditions in the longwall in terms of the methane hazard, as it moves the zone of high methane concentrations away from the longwall working to the goaf [4,7-9].

Safe and productive mining requires the knowledge of a number of interrelated phenomena, in particular the processes of methane migration and longwall face ventilation [10]. Computer

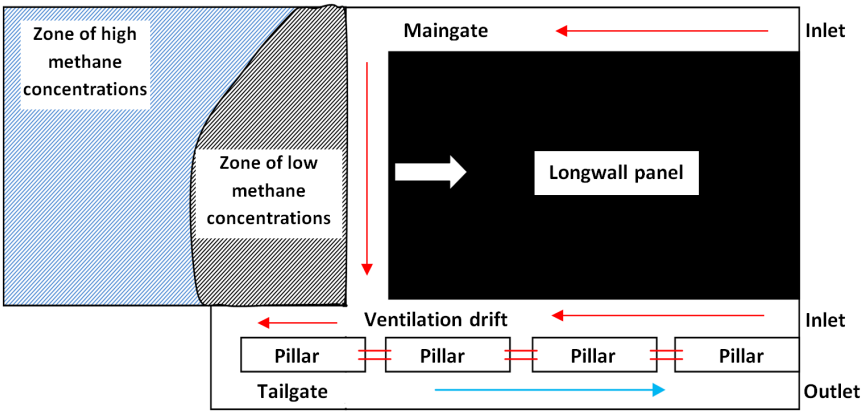

Fig. 2. Method of longwall face ventilation by means of "short Y"

simulations, using the tools of Computational Fluid Dynamics (CFD), in particular the finite volume method, are increasingly widely used research tools [13]. Examples of applications may be found in some papers [6] and the paper [14-16] contain a more complete literature review of this topic.

This paper presents the process of numerical model development and preliminary simulation results for the issue of a shearer operation at a mining longwall ventilated by means of the "short Y" method under methane hazard conditions. The research goal of the article is to develop the 3D numerical method of air and methane flow modelling on the shape reflecting the geometry of the longwall with caving with the use of the CFD method. The research gaps in the article are to fill the methodology development of 3D simulations of methane distribution in the working of a longwall taking into account detailed elements such as shearer, powered roof support and arch yielding support. In the literature, it can be found that the algorithms or the numerical models based on the 2D numerical method [2-4,12] that operate at the empirical constant usually defined under a laboratory or an in-situ condition. The presentation of the model formulation process is justified by the fact that the reliability of the modelling results to a large degree depends on the adopted methodology and the quality of information, including that related to boundary conditions, especially the methane inflow. In the considered case, it may be useful to apply verified methods for forecasting methane hazards. The paper presents the way how, based on methods widely used in the Upper-Silesian Coal Basin and the methane inflows, were determined for specific mining and geological conditions of longwall Z-11, ventilated by means of the "short Y" method.

2. Theoretical background

The release of methane from a mined seam may be characterised by a stream of methane released from the extracted coal, from the longwall face, and as a result of the mined seam destressing. The mined coal seam features a methane-bearing capacity lower than the original methane-bearing capacity of the seam. The carried out research allowed the determination of the degree of methane content reduction η_s concerning its primary methane-bearing capacity M_0 (Fig. 3).

The curves in Fig. 3 were determined based on the results shown in [11]. In Fig. 3, for example, for the exploited seam with the value of primary methane-bearing capacity 6 m^3 CH_4/Mg_{csw}, the total value of the coal degassing degree of the seam (h), amounting to 48.34%, and the value of the degassing degree of the seam during shearer mining (h_s), amounting to 27.75%, are mapped on the ordinate axis [11].

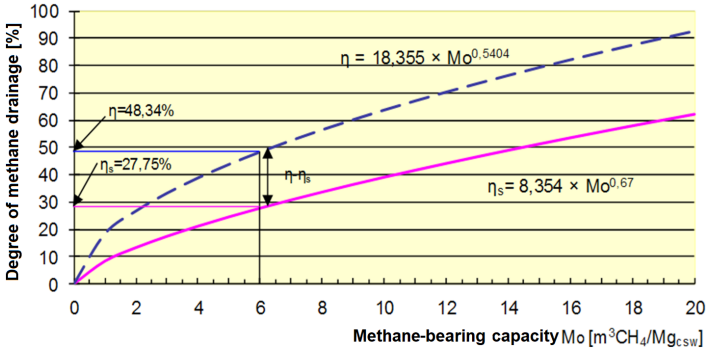

Fig. 3. The degree of methane drainage η_s of the mined seam after cutting with a shearer, versus its methane-bearing capacity M_0

The volumetric methane stream released from the mined seam during one cutting cycle is directly proportional to the volume of mined coal, its original methane-bearing capacity M_0, the degree of its methane drainage η_s and inversely proportional to the time of mining cycle "t", and is calculated by using the formula [11]:

$$\dot{V}_{\acute{s}c}^{u} = \frac{L_s m_e \gamma z M_0 \eta_s}{100t} \tag{1}$$

where:

- η_s — degree of methane drainage during coal cutting, %;
  $\eta_s = 8.354\ M_0^{0.67}$
- L_s — longwall length, m;
- m_e — height of the mined longwall, m;
- γ — coal density, Mg/m^3;
- z — shearer cut width, m;
- M_0 — primary methane-bearing capacity of the mined seam, m^3 CH_4/Mg_{csw};
- η — degree of mined seam methane drainage, %;
- t — time of one cutting cycle, min;
- $\dot{V}_{\acute{s}c}^{u}$ — stream of methane volume released to the longwall per one cutting cycle, m^3CH_4/min.

The amount of methane released to the longwall face may be expressed by the relationship:

$$V_{\acute{s}c} = \dot{V}_{\acute{s}c}^{u} + \dot{V}_{\acute{s}c}^{oc}\ [\mathrm{m^3CH_4/min}] \tag{2}$$

Where $\dot{V}_{śc}^{u}$ is the stream of methane released from the mined coal seam during its cutting $\dot{V}_{śc}^{u}$, while $\dot{V}_{śc}^{oc}$ is the stream of methane released from the longwall face. The amount of methane released from nearby situated seams to the longwall depends on the distance of their deposition $h_{\min}$ expressed by the formula [11]:

$$h_{\min} = 1.73\ (l_s + l_c) \tag{3}$$

where:

l_s — width of the longwall working space, m;
l_c — distance of the abutment pressure existence ahead of the longwall front, m;
1.73 — value of the desorption angle tangent

Fig. 4 presents a possibility of methane inflow to the longwall from nearby situated underworked and overworked seams. The release of methane to the longwall from nearby situated underworked and overworked seams may only occur if they are deposited at a distance of $h_{\min} > a$ and/or $h_{\min} > b$ (Fig. 4).

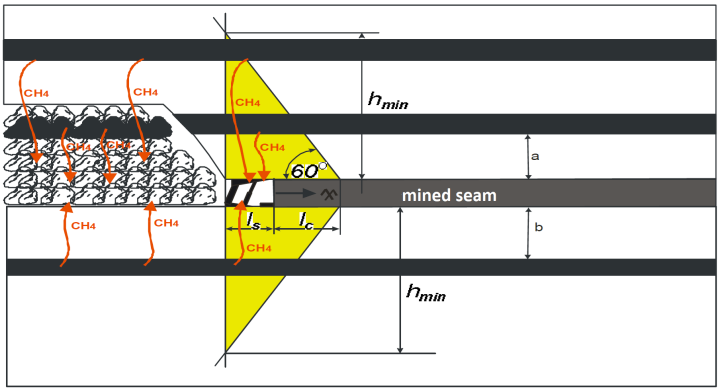

Fig. 4. Model of methane inflow to the longwall from nearby situated underworked and overworked seams

The value of ventilation methane content is calculated from formula (4):

$$\Delta V_{\mathrm{CH_4}}^{śc} = 0.01(c_2 - c_1)\ Q_{śc} \tag{4}$$

where:

$Q_{ść}$ — quantity of air flowing through the longwall $Q_{ść} = 0.8\ Q_{pow}$;
Q_{pow} — quantity of air supplied to the longwall, m^3/min;
c_1 — methane concentration at the longwall inlet, %;
c_2 — methane concentration at the longwall outlet, %.

The increase $\Delta \dot{V}_{\mathrm{CH_4}}^{śc}$ calculated from formula (4), if there is no cutting, allows to determine a total value of methane streams released to the longwall, including the component $\dot{V}_{śc}^{oc}$ from the longwall face, formula (1), and the methane inflowing directly to the longwall from nearby situated underworked and overworked seams.

If we add methane supplied with intake air to the ventilation volume $\Delta \dot{V}_{CH_4}^{śc}$ of methane released to the longwall, calculated from formula (4), we obtain ventilation methane-bearing capacity of the longwall acc. to formula (5):

$$\Delta V_{CH_4}^{wylot\ ściany} = 0.01\, c_2\ \ Q_{śc}\ \ [\mathrm{m^3 CH_4/min}] \tag{5}$$

Methane released to the goaf is referred to as the absolute methane-bearing capacity of the longwall goaf $\Delta \dot{V}_{CH_4}^{zr}$. For the majority of longwalls the value of the volumetric stream of methane released to the goaf is the biggest component among all sources of methane release to the longwall environment. If the methane drainage is not applied, the methane-bearing capacity of the longwall goaf $\Delta \dot{V}_{CH_4}^{zr}$ migrates entirely to the air flowing through the area of mining.

If methane drainage is used, the stream of methane released to the goaf $\Delta \dot{V}_{CH_4}^{zr}$ separates into the volumetric stream of methane $\dot{V}_{CH_4}^{zr,\ odm}$ captured by methane drainage and $\dot{V}_{CH_4}^{zr,went}$ the volumetric stream of methane $\dot{V}_{CH_4}^{zr,went}$ released from the goaf to ventilation-active workings, $[\mathrm{m^3\ CH_4/min}]$.

$$\dot{V}_{CH_4}^{zr} = \dot{V}_{CH_4}^{zr,\ odm} + \dot{V}_{CH_4}^{zr,went} \tag{6}$$

The amount of methane captured by the goaf methane drainage shapes the value of methane stream discharged to the ventilation air of the mining area, calculated by formula (7), rearranging formula (6).

$$\dot{V}_{CH_4}^{zr,went} = \dot{V}_{CH_4}^{zr} - \dot{V}_{CH_4}^{zr,\ odm} \tag{7}$$

3. Numerical model

The construction of a spatial model is the basic condition to perform computations forecasting the methane concentration distribution at longwall Z-11. The longwall Z-11 was mined in the "short Y" system. This method of longwall ventilation consists in supplying intake air by the Maingate, refreshing the air at the longwall outlet by so-called ventilation drift driven along unmined part of the coal panel. The return air is directed behind the front of the Z-11 longwall, along the goaf to the ventilation cross-cut connecting the ventilation roadway with the tailgate. The "short Y" method moves away dangerous methane accumulations in the goaf from the longwall face, redirecting the goaf methane migration to the adjacent to goaf part of the ventilation drift.

Fig. 5 presents visually the "short Y" ventilation method used at longwall Z-11.

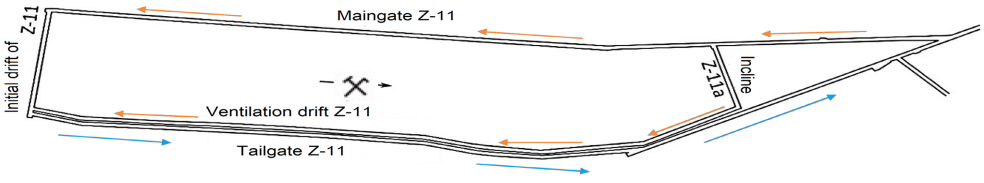

Fig. 5. A view of the longwall galleries prior to the start of excavation, based on the map of seam 408/1

A CFD numerical model of longwall Z-11 in seam 408/1 was developed in the following order:

- mining and geological conditions in the area of longwall Z-11 mining panel in seam 408/1 have been analysed,
- ventilation method has been analysed in terms of determination of flow directions and quantities in the workings and air and methane migration directions in the longwall goaf (Fig. 5),
- assumptions for the development of a CFD numerical model have been adopted,
- inlet velocity and turbulence profiles for both the Maingate and the Ventilation Drift have been obtained from auxiliary flow simulations,
- a set of numerical simulations of the air and methane propagation in workings of longwall Z-11 and adjacent goaf have been performed.

3.1. Geometry

A geometrical model of the longwall mining panel has been developed for longwall Z-11 in seam 408/1 (Fig. 6), taking into account the "short Y" method and parameters of longwall Z-11 ventilation, considering migration of air and methane through the goaf to the air roadway. Longwall Z-11 was equipped with a shearer with two cutting heads, 1850 mm in diameter, which enabled making a cut up to 0.8 m wide. Seam 408/1, including intrusions, was 2.41 m thick. The area of the Maingate and Tailgate as well as the Ventilation drift is 17 m^2. The area of the working of a longwall panel Z-11 is 16.5 m^2.

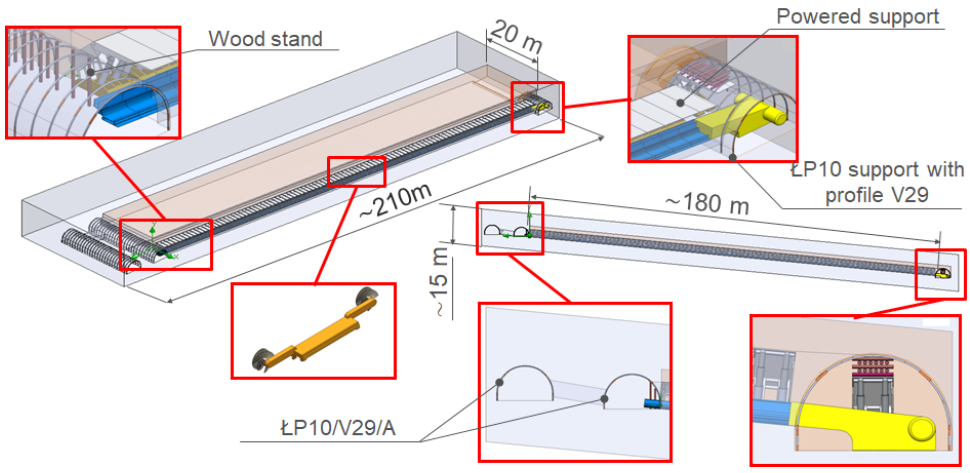

Fig. 6. View of spatial model of longwall Z-11 developed for numerical simulations

For the case study, three shearer positions at longwall Z-11 in seam 408/1 have been selected: at the beginning of longwall working Z-11 (shown in Fig. 7a), at the mid-length of the longwall working (shown in Fig. 7b) and at the longwall working end (shown in Fig. 7c), to consider the effect of its advance on flow and migration of methane (see . Fig. 7).

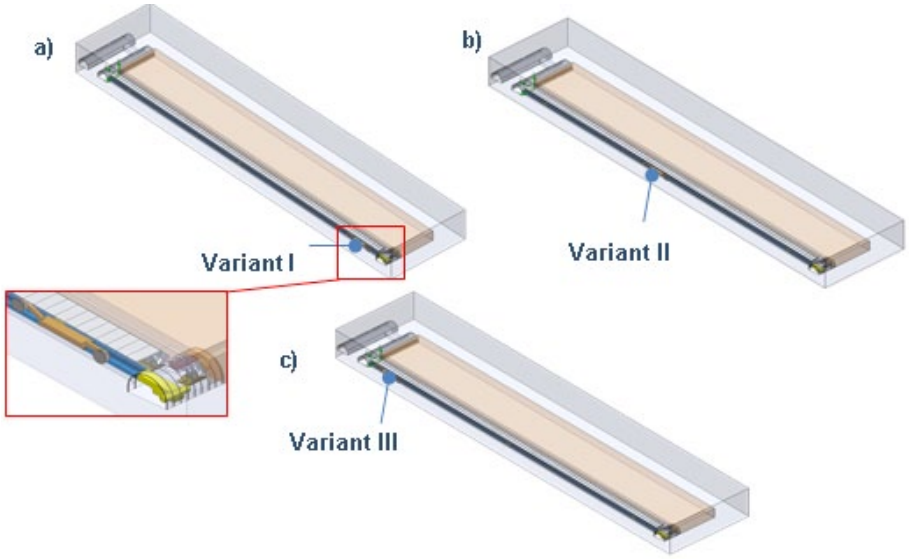

Fig. 7. Variants of shearer position: a – at the beginning of longwall Z-11 face,
b – in the middle of longwall Z-11 face length, c – at the face end of longwall Z-11

3.2. Numerical grid

In order to ensure that the results obtained from numerical calculations are adequate, it is crucial to use a correctly refined mesh. Fig. 8 illustrates the mesh refinement study on the volume flow rate results in the numerical model. The measured volume flow rate of the fluid was taken at the outlet of the longwall panel model.

The results of the four mesh densities were compared in Table 1

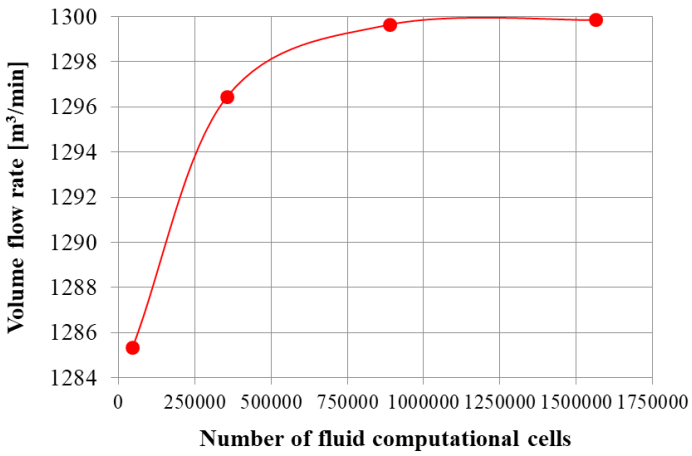

Fig. 8. Convergence of results in the numerical grid refinement study of longwall panel Z-11

TABLE 1

Results of numerical grid refinement study

No	Mesh quality	Number of fluid computational cells	Volume flow rate [m^3/min]
1	coarse mesh	45.716	1285.34
2	normal mesh	355.428	1296.45
3	fine mesh	889.123	1299.65
4	very fine mesh	1,565,236	1299.85

It can be observed in Table 1 that the coarse and normal mesh forecast has less accurate volume flow rates, but the fine and very fine mesh forecast similar results. In this case, it was decided that the mesh in the numerical model would contain above the 889,123 computational cells according to the convergence study results. The value of refinement in Fig. 9 is the result of grid sensitivity analysis, where the solver improves and refines the mesh of the longwall panel without active user intervention during the numerical calculations.

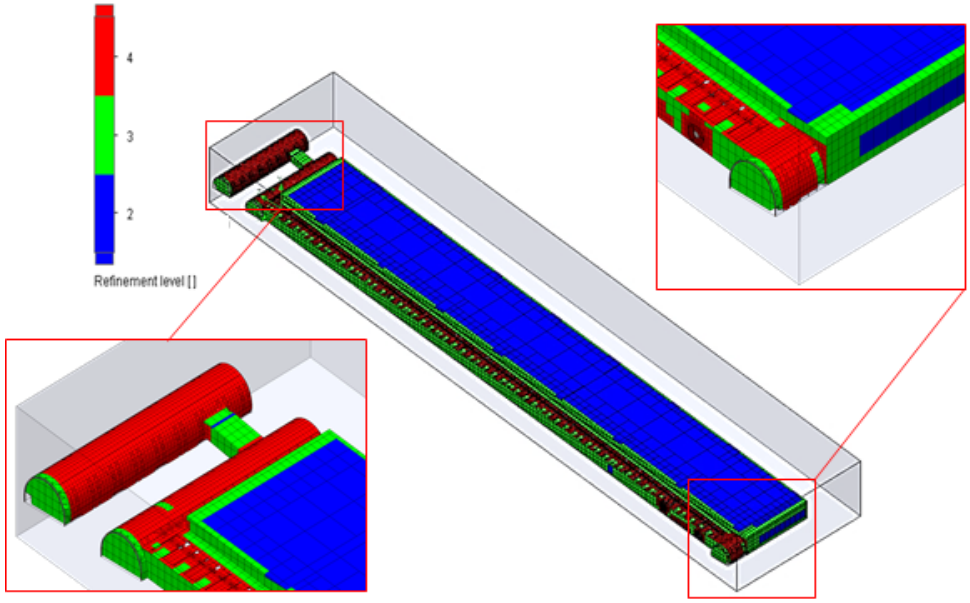

Fig. 9. Numerical grid of longwall panel Z-11

3.3. Assumptions

The flow at the longwall is highly turbulent. In particular a classical *k*-epsilon turbulence model has been applied. Solving a flow problem with this model comes down to determining the value of turbulent viscosity μ_t using turbulence kinetic energy k and dissipation rate ε related to the energy dissipation, by solving the k and ε transport equations. The detailed description of this model is available in SolidWorks Flow Simulation references [17]. The goaf's properties in numerical model (porous media) were defined by the expression:

$$K = \frac{grad\,(P)}{pV} = \frac{\Delta p \cdot S}{\dot{m} \cdot L} \tag{13}$$

where ΔP is the pressure difference between the opposite sides of a parallelepiped porous media, $\dot{m}$ is the mass flow rate through the porous media and S and L are the body cross-sectional area and length. As the "short Y" reduces interactions of goaf and longwall, a relatively simple model of constant, isotropic permeability has been selected. The equations have been numerically solved with the finite volume method.

4. *In-situ* tests

In-situ tests were carried out at longwall Z-11 in the mined seam 408/1 and partly in seam 407/3. On the day of measurements, the longwall length was equal to 119 sections of powered support. The record was recorded every 6 seconds. The accuracy of the measuring instruments was ±0.1% CH_4 in the subrange 0÷2.5% CH_4 and 10% of indication above 2.5% CH_4.

4.1. Measurements of methane concentration changes along the face of longwall Z-11

Locations of methane sensors (yellow, numbers 117, 137, and 132) and also locations of additional sensors with numbers 421, 115, 109, and 133 are marked on the spatial diagram of the longwall Z-11 area (Fig. 10). The analysis comprised 2127 recorded readings of automated methane monitoring and control system.

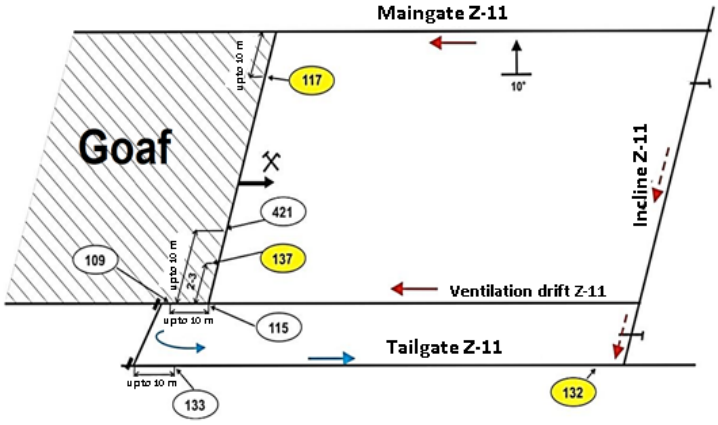

Fig. 10. Arrangement of methane monitoring and control sensors in the area of longwall Z-11, seam 408/1

Figs. 11-14 present concentration values of methane released after the end of mining, where:

– methane concentration at longwall Z-11 face end after the end of mining is 0.7%, going down to 0.2% within a dozen or so hours,

– immediately after the end of mining the uncovered coal solid of the mined seam is drained of methane within the mentioned above interval,
– after this transient period, the recorded increase in the methane concentration between the air inlet and outlet from longwall Z-11, equal to 0.2%, can be used to evaluate the methane migration from nearby situated undermined and over mined seams and from the Z-11 longwall face.

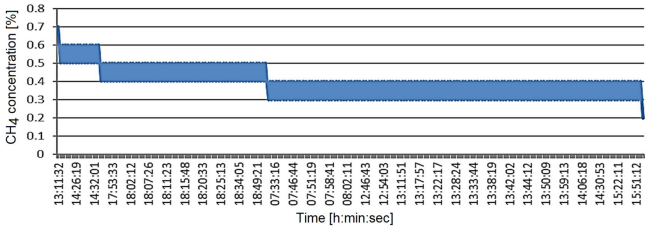

Fig. 11. Readings recorded by a sensor of automated methane monitoring and control system on 02/02/2019

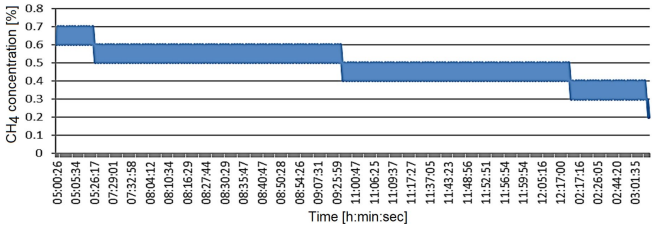

Fig. 12. Readings recorded by a sensor of automated methane monitoring and control system on 09/02/2019

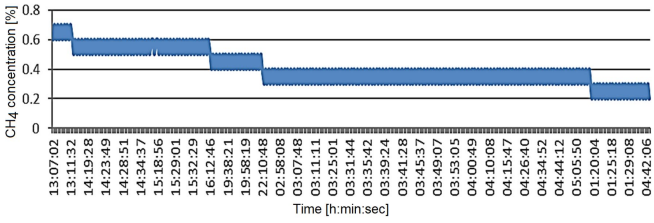

Fig. 13. Readings recorded by a sensor of automated methane monitoring and control system on 16/02/2019

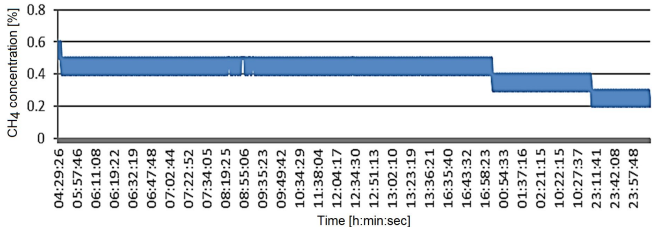

Fig. 14. Readings recorded by a sensor of automated methane monitoring and control system on 23/02/2019

The analysis of methane concentrations based on methane sensors 117 and 421 at the inlet and outlet from the longwall allowed us to calculate that on average 4.1 m^3 CH_4/min was released from the longwall face.

TABLE 2

Analysis of methane concentrations at longwall Z-11

		2 & 3 Feb. 2019	9 & 10 Feb. 2019	16 & 17 Feb. 2019	23 & 24 Feb. 2019	Averaged values
Time without mining	min	2388	3228	2441	2470	**2632**
Average methane concentration	%	0.38	0.34	0.35	0.29	**0.34**
Amount of released methane	m^3	7218	8780	6777	5799	**7144**
Ventilation methane-bearing capacity of the longwall	m^3/min	3.00	2.72	2.78	2.35	**2.71**

The value of released methane refers to the working days without considering the failures and technological breaks, as well as breaks between shifts. On working days, the average ventilation methane-bearing capacity at the longwall face was 4.6 m^3 CH_4/min. The analysis of instantaneous values of absolute ventilation methane-bearing capacity at longwall Z-11, presented in Fig. 15, shows the maximum instantaneous values of absolute ventilation methane-bearing capacity that were 12 m^3 CH_4/min, which is about four times higher than the average, showing direct effects from mining.

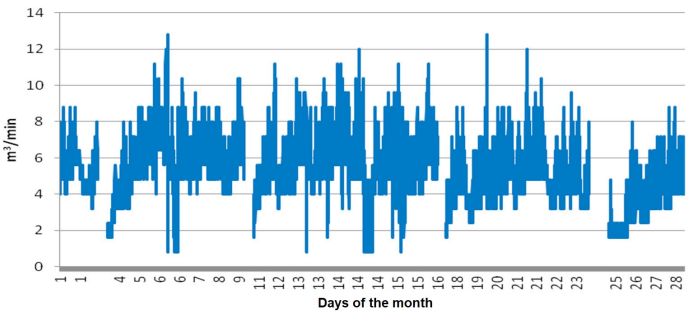

Fig. 15. Ventilation methane-bearing capacity - instantaneous at longwall Z-11

4.2. Measurements at the cross-section of longwall Z-11 face

The routine ventilation survey and mine monitoring data have been supplemented with results of dedicated in-situ measurements. Unique SOM2032 probes providing simultaneous velocity and methane concentration point measurements have been applied. Ten SOM2032 methane-anemometers recorded velocity and concentration distribution approx. 20 m from the longwall face end.

Locations of methane-anemometers at the measuring cross-section are marked in Fig. 16. Circles mark the actual position of the methane-anemometer. Labels contain the device number – in capital letters and the position on the x and y-axis – in small letters. Axis x is the horizontal

axis, y is the vertical one. The origin of the system of coordinates is situated on the sole plate of the powered support section. Fig. 17 presents measurement results of changes of air velocity and methane concentration in the air flowing through the studied cross-section of the longwall face.

From graphs in Fig. 17, the average air velocity value at the working cross-section was 1.8 m/s, whilst an average value of methane concentration in the air was 0.20%.

Fig. 16. Measuring cross-section, longwall Z-11, face end. Section No 99/119

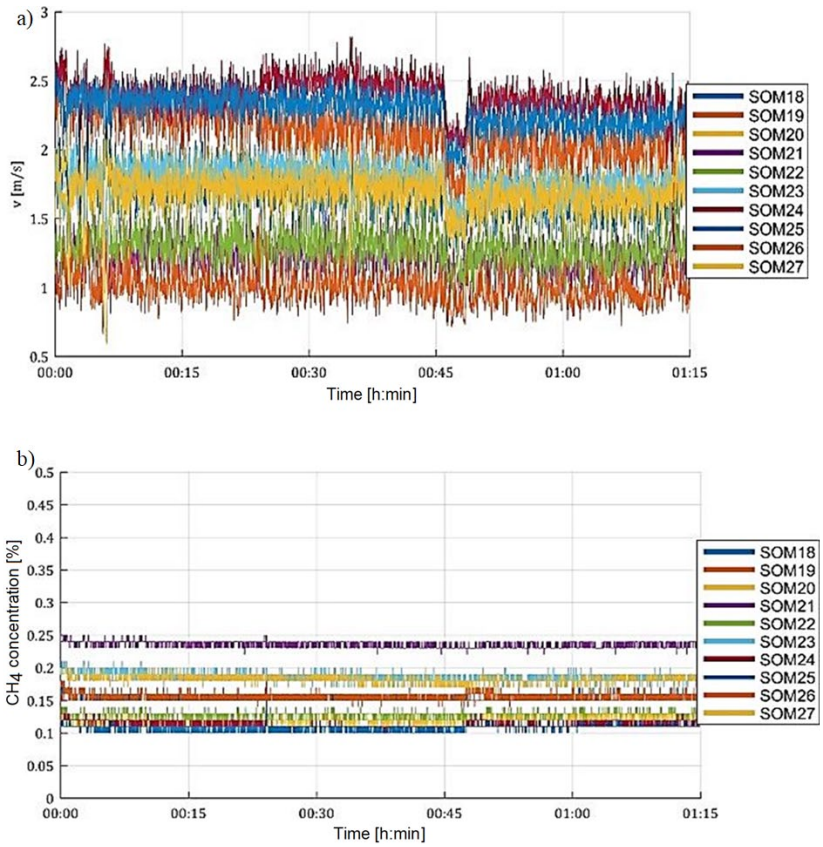

Fig. 17. Registrations of velocity (a) and methane concentration (b) at the measuring cross-section of the longwall face

5. Model studies

Before starting the numerical simulations of methane propagation at longwall Z-11, auxiliary simulations have been performed to evaluate inlet velocity and turbulence profiles at galleries supplying the air to the longwall.

5.1. Analysis of air velocity profile development at inlet drifts

Data available for the inlet drifts specified flow quantities only due to their length the developed velocity profiles could be expected. Auxiliary models of both Maingate and Ventilation Drift sections have been created. If around the inlet to the longwall face the inflowing air features an unknown profile, it is required to carry out a simulation of the airflow on a sufficiently long section to obtain a profile close to a fully developed one. The length of velocity profile forming was determined based on models in both galleries, through which the air is supplied to the face of longwall Z-11. The lengths and flow quantities are taken from the ventilation survey and are as follows:

- 300 m^3/min of intake air is supplied by the Ventilation Drift, 50 m long (Fig. 18),
- a stream of intake air volume of 1000 m^3/min is supplied to longwall Z-11 through the Maingate, 100 m long (Fig. 19).

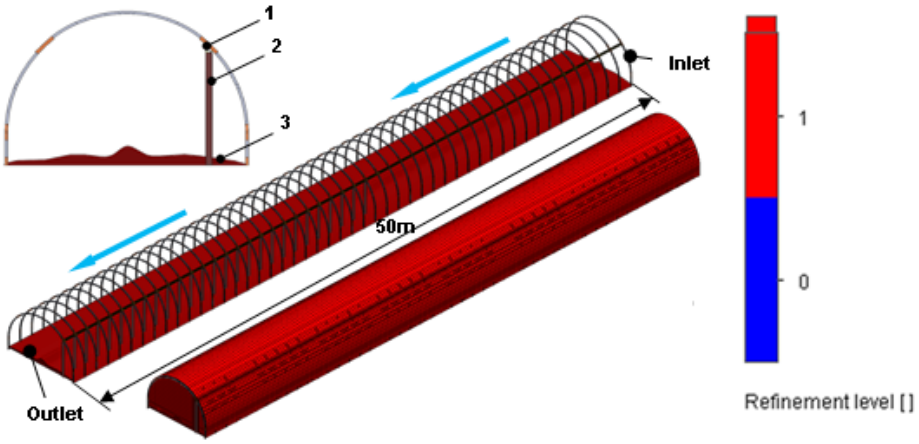

Fig. 18 Spatial model and numerical grid of longwall Z-11 Ventilation Drift: 1 – steel crown runner, 2 – wooden prop, 3 – floor uplift, 0.4 m high

Fig. 20 presents results of air velocity profile changes along the studied sections of galleries in the form of graphical maps.

It is possible to observe that the air profile has divided into three layers. The first layer of viscous fluid is at the walls, roof, and floor of the roadway, where the velocity reaches a zero value. The second boundary layer in which the air stream features a smaller velocity as against the velocity in the axis of top and bottom roads (so-called third layer of fluid). The third area of flow is a developed and a shaped layer of fluid, in which the air increases the maximum velocity

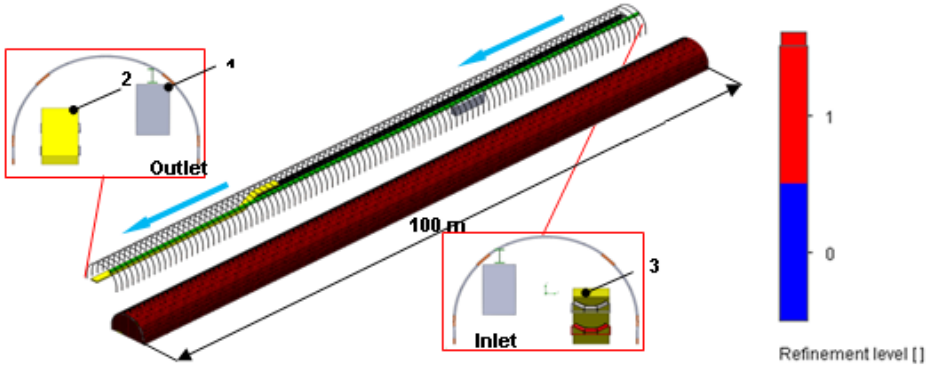

Fig. 19. Spatial model and numerical grid of longwall Z-11 Maingate: 1 – transformer, 2 – GROT chain conveyor, 3 – belt conveyor

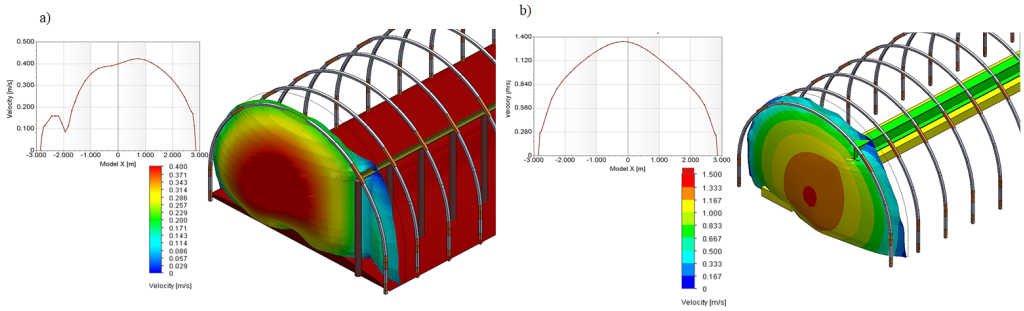

Fig. 20. Air velocity profile at the outlet from the Ventilation Drift (a) (Z-11 air roadway – Fig. 12) and the Maingate (b) (Z-11 roadway – Fig. 12) of longwall Z-11

values to maintain a constant value of volumetric stream set at the inlet to the top and bottom road. In the bottom road, the maximum value of air velocity was approx. 0.5 m/s (Fig. 19), while in the top road approx. 1.4 m/s (Fig. 20b). Fig. 21 presents the results of the analysis of the air velocity profile forming length in the studied top and bottom roads in YZ and XZ planes.

The obtained velocity profiles at the outlet both gateroads (Fig. 20) are a boundary condition of the velocity of air supplied at the inlet to the model of longwall Z-11 face.

5.2. Boundary conditions

The input assumptions for ventilation parameters in the CFD model are as follows:

- air at the amount of 1000 m^3/min is supplied to longwall Z-11 through the Maingate,
- air at the amount of 200 m^3/min migrates along longwall Z-11 to the goaf,
- 300 m^3/min of intake air are supplied by the Ventilation Drift to the outlet of longwall Z-11,
- yield of return air is 1300 m^3/min,
- methane concentration in the stream of air supplied through the bottom road to longwall Z-11 is 0.0% of methane,

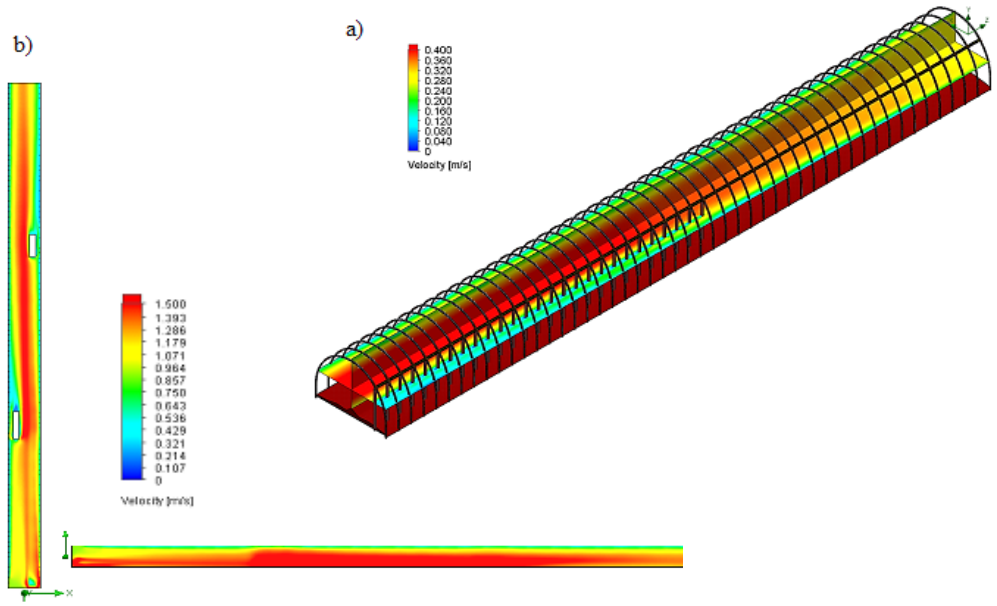

Fig. 21. Air velocity profile along the length of Ventilation Drift (a) and Maingate (b) of longwall Z-11 in XZ and YZ planes

– during cutting, the degassing coal causes an increase in the methane concentration in the intake air to a value of 0.1%,
– methane from nearby situated seams and underworked and overworked coal layers inflows to the longwall face and goaf.

The calculated volumetric streams of methane inflowing from nearby situated seams amount to:

– 4.67 m^3 CH_4/min inflows to the goaf in the section from the longwall to the ventilation cross-cut,
– 1.03 m^3 CH_4/min inflows to the longwall face.

TABLE 3

Forecast methane release to the longwall in a cutting cycle at longwall Z-11

Methane content of seam 408/1 coal M_0	**Degree of methane drainage η_s – acc. to (2)**	**Forecast amount of methane released during a cutting cycle – acc. to formula (1)**			
		80	**100**	**120**	**140**
m^3 CH_4/Mg_{csw}	**%**	**m^3 CH_4/min**			
3.5	19.34	3.71	2.86	2.47	2.12
4.0	21.15	4.63	3.70	3.09	2.65
4.5	22.88	5.64	4.51	3.76	3.22
5.0	24.56	6.72	5.38	4.48	3.84
5.5	26.18	7.88	6.31	5.25	4.52

For parameters of longwall Z-11, i.e. its length of 180 m, face height of 2.41 m, 0.66 m shearer cut width, calculations were carried out for four variants of a single cutting cycle performance (80, 100, 120, and 140 minutes). Table 3 specifies calculation results for methane release during cutting by the shearer. The line referring to mining by the shearer of a seam with 5 m^3 CH_4 / Mg_{csw}, i.e. an averaged value for the panel in seam 408/1, has been highlighted in yellow in Table 3.

5.3. Results of simulations for longwall Z-11 face

Figures 22, 23, and 24 present results of CFD simulations, related to variants of the shearer position, namely:

- **variant I** describes the shearer position at the beginning of the longwall Z-11 face,
- **variant II** describes the shearer position mid-length of the longwall face,
- **variant III** describes the shearer position at the face end.

Figs 22a, 23a, and 24a present a diagram of the sensor arrangement in the numerical model. Figs. 22b, 23b, and 24b show the distribution of methane concentration depending on the position of the measuring sensors. Figs. 22c, 23c, and 24c present maps of methane concentration distribution at the face.

Results presented in Fig. 22b shows that for the case of shearer position at the beginning of the longwall face (Variant I – Fig. 8a), the obtained calculations forecast a possibility of methane concentration increase from 0.09% for the beginning of the face (sensor/measuring point 1 – Fig. 22a) to 0.61% measured at the face end (sensor/measuring point 6 – Fig. 22a). For the case of mid-face shearer position (Variant II – Fig. 8b), the simulation results (Fig. 23b) forecast an increase in the methane concentration from 0.09% for the beginning of the face (sensor/measuring point 1 – Fig. 23a) to 1.05% measured at the face end (sensor/measuring point 6 – Fig. 22a).

Results presented in Fig. 24b shows that, for the case of shearer position at longwall Z-11 face end (Variant III – Fig. 8c), the obtained numerical calculations forecast a possibility of

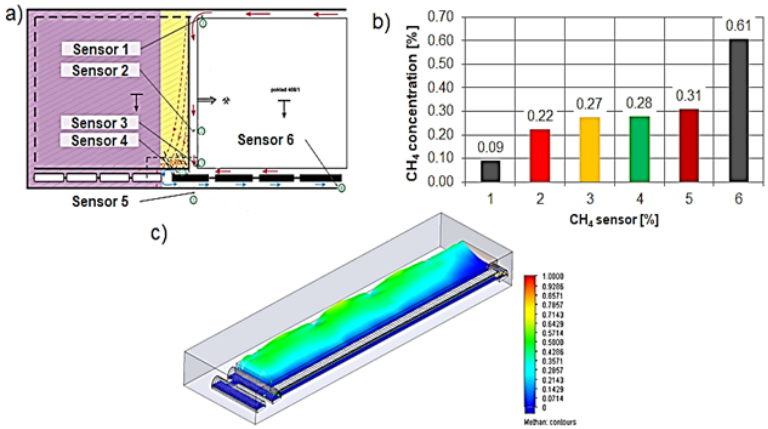

Fig. 22. The forecast distribution of methane concentration changes for variant I of the shearer position: a – diagram of sensors arrangement, b – graph of methane concentration changes distribution, c – map of methane mass share

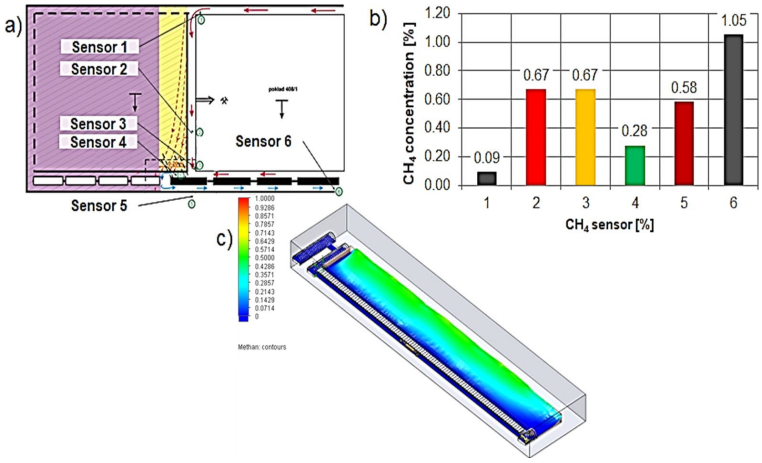

Fig. 23. The forecast distribution of methane concentration changes for variant II of the shearer position: a – diagram of sensors arrangement, b – graph of methane concentration changes distribution, c – map of methane mass share

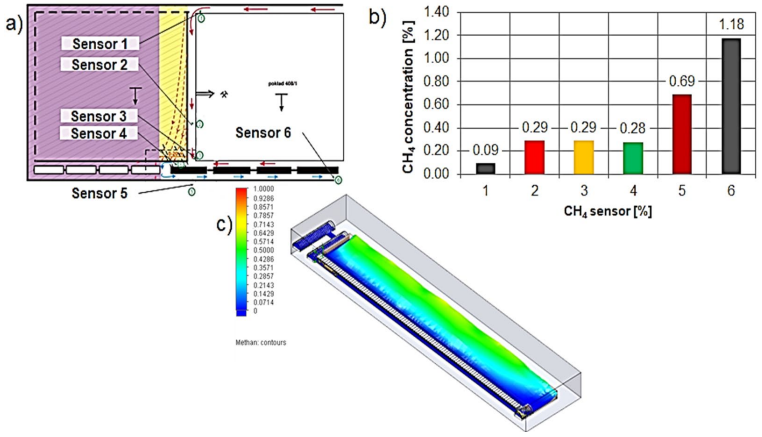

Fig. 24. The forecast distribution of methane concentration changes for variant III of the shearer position: a – diagram of sensors arrangement, b – graph of methane concentration changes distribution, c – map of methane mass share

methane concentration increase from 0.09% for the beginning of the face (sensor/measuring point 1 – Fig. 24a) to 1.18% measured at the face end (sensor/measuring point 6 – Fig. 24a).

5.4. Validation of results

Fig. 25 presents the methane concentration changes obtained from the simulation and from the in-situ measurements at the longwall face in the actual and simulated shearer position at the beginning of the longwall face (variant I).

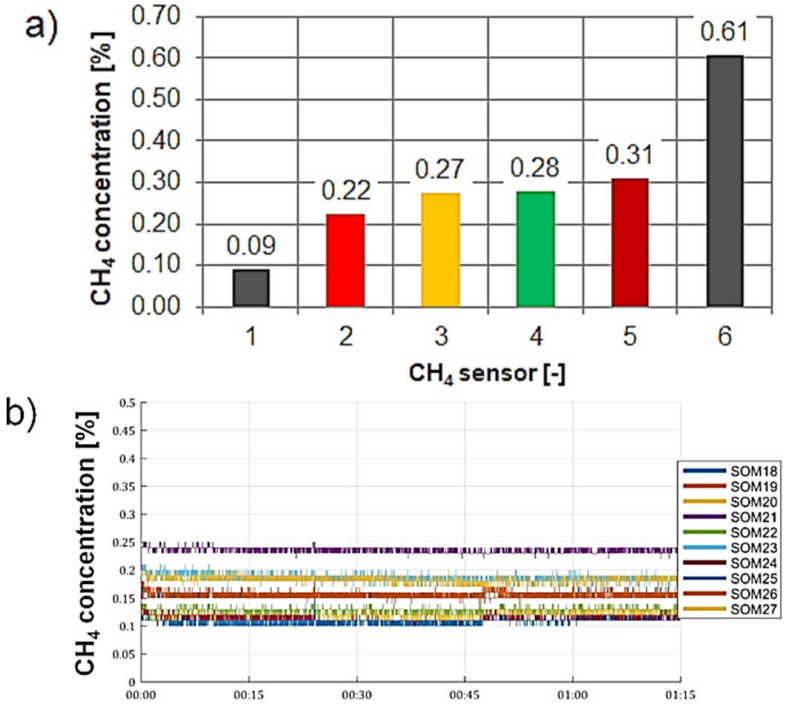

Fig. 25. Distribution of methane concentration changes at the cross-section of the longwall face obtained from numerical calculations (a) and from measurements (b)

The analysis of graphs in Fig. 25 shows that for the shearer position at the beginning of the longwall face (variant I), an average value of methane concentration from numerical calculations was 0.23%, whilst the value from in-situ measurements, done for a similar position of the shearer was 0.20% (the sensor SOM20 in Fig. 25b), which gives a difference in calculations error of approx. 13%.

The analysis of graphs in Fig. 26 shows that for the shearer position at the beginning of the longwall face (variant I), an average value of air velocity from numerical calculations was 2.0 m/s, while from in-situ measurements of 1.75 m/s (the sensor SOM20 in Fig. 26b), which gives a difference in calculations error of approx. 12%.

Table 4 compares the CH_4 measurements obtained during the in situ test and CFD simulations. Relative error was used as an approximation error between the values.

TABLE 4

Results of the velocity and CH_4 measurements comparison obtained during in-situ tests and CFD calculations (for average values)

In-situ		**CFD**		**Relative error**	
Velocity [m/s]	**CH_4 concentration [%]**	**Velocity [m/s]**	**CH_4 concentration [%]**	**Velocity [%]**	**CH_4 concentration [%]**
1.8	0.175	2.0	0.196	11	12

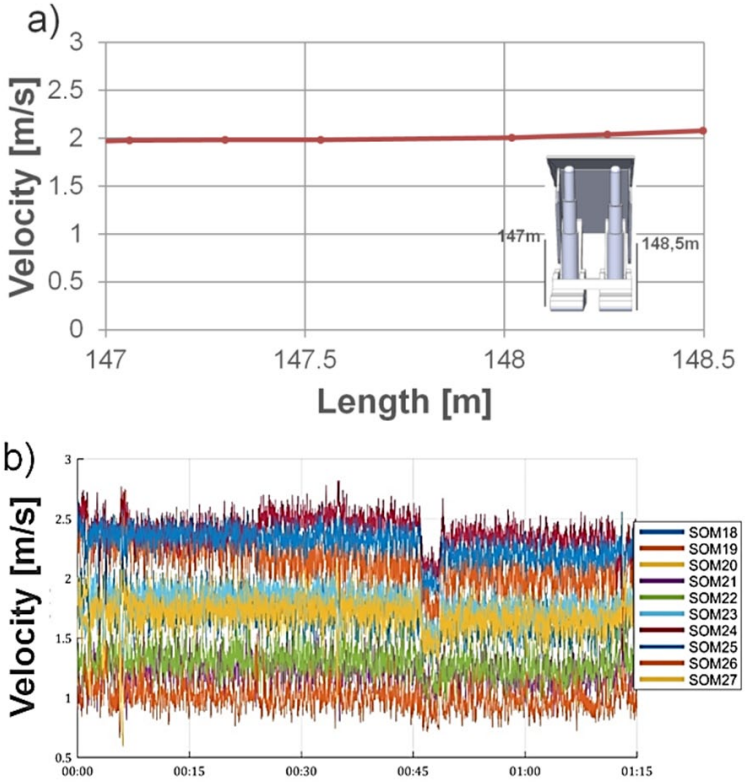

Fig. 26. Distribution of air velocity changes at the cross-section of the longwall face obtained from numerical calculations (a) and from measurements (b) (section No 99/119)

It can be observed that the relative error between the velocity value obtained from the in-situ tests and the numerical model is 11%. However, the relative error between methane concentration values obtained from the in-situ tests and the numerical model is 12%. The difference between the in-situ and the numerical simulation results were caused by setting the permeability and porosity variations of the goaf, which cannot be monitored in-situ, which were described by a semi-empirical relationship.

6. Summary and conclusions

The adopted method of longwall Z-11 ventilation by means of "short Y" results in the methane migration from the goaf (in the section longwall Z-11 – ventilation cross-cut) to the air roadway. The estimated methane stream value allowed the modelling of its inflow from the goaf to the air roadway behind the longwall Z-11 front. Calculation results of methane streams inflowing to the longwall and goaf are the input data to carry out simulation calculations by the numerical CFD of longwall Z-11. The information on the amount of methane stream inflowing as a result of

methane drainage of nearby situated underworked and overworked seams was indispensable to perform calculations. The carried out computations allowed the calculated values of volumetric streams of released methane, i.e.:

- methane released from the mined seam 408/1 during cutting, in accordance with Table 1,
- to the goaf of longwall Z-11 in a section 20.5 m long (i.e. an average distance between cross-cuts), which is 4.67 m^3 CH_4/min.,
- to the face of longwall Z-11, 4.5 m wide, from nearby underworked and overworked seams, which is 1.03 m^3 CH_4/min.

The obtained results of model and experimental studies allow to draw the following conclusions:

- the development of a CFD numerical model for the longwall ventilated by means of the "short Y" method enabled to analyse of the variant calculations of methane concentration distribution in the workings of the mined area,
- results of numerical calculations of the methane concentration distribution and the air velocity values are comparable with results of in-situ measurements, which confirms the correctness of assumptions made for the CFD numerical model,
- the adopted numerical method provides information about 3D velocity fields of the air flow and methane concentrations in the longwall workings and the adjacent goaf,
- the carried out simulations confirm a significant impact of the shearer's position on the distribution of methane concentration at the longwall face, and hence on the development of gas conditions at the longwall face,
- the developed numerical model provides possibilities to forecast the methane concentration distribution depending on the shearer's position for the given geometry of the longwall face,
- the developed methodology and model may be useful for analyses comprising not only different shearer's positions but also various phases of the longwall mining, in particular a variable length of "short Y" section,
- the results of the developed numerical model may emerge useful at the stage of underground mining designing. They can also resolve several issues which can occur during the mining.

Acknowledgment

The study was carried out as part of the PICTO research project titled "Production Face Environmental Risk 403 Minimization in Coal and Lignite Mines", No. 800711, financed by the Research Programme of the Research 404 Fund for Coal and Steel (RFCS) and Polish MNiSW W93/FBWiS/2018.

References

[1] S. Prusek, E. Krause, J. Skiba, Designing coal panels in the conditions of associated methane and spontaneous fire hazards **30** (4), 525-531 (2020). DOI: https://doi.org/10.1016/j.ijmst.2020.05.015

[2] W. Dziurzyński, A. Krach, T. Pałka, Shearer control algorithm and identification of control parameters. Arch. Min. Sci. **63** (3), 537-552 (2018).

[3] W. Dziurzyński, A. Krach, J. Krawczyk, T. Pałka, Numerical Simulation of Shearer Operation in a Longwall District. Numerical Simulation of Shearer Operation in a Longwall District. Energies **13**, 5559 (2020). DOI: https://doi.org/10.3390/en13215559

[4] E. Krause, A. Przystolik, B. Jura, Warunki bezpieczeństwa wentylacyjno-metanowego w ścianach o wysokiej koncentracji wydobycia. XXI Międzynarodowa Konferencja Naukowo-techniczna Górnicze Zagrożenia Naturalne. 6-8.11.2019 r., Jawor k. Bielska Białej.

[5] A. Walentek, T. Janoszek, S. Prusek, A. Wrana, Influence of longwall gateroad convergence on the process of mine ventilation network-model tests. International Journal of Mining Science and Technology **29**, (4), 585-590 (2019).

[6] A. Juganda, J. Brune, G. Bogin, J. Grubb, S. Lolon, CFD modeling of longwall tailgate ventilation conditions. In: Proceedings of the 16th North American mine ventilation. Golden, CO; 2017.

[7] E. Krause, Z. Lubosik, Wpływ koncentracji wydobycia podczas eksploatacji pokładów silnie metanowych na wydzielanie się metanu do środowiska ścian. 9th International Symposium on Occupational Heat and Safety Petrosani Rumunia. October 3rd 2019 r.

[8] E. Krause, J. Skiba, B. Jura, Overview of Ventilation Characteristic, Practices and regulations in Poland. XXVIII Szkoła Eksploatacji Podziemnej, Kraków, 25-27.02.2019 r. https://unece.org/fileadmin/DAM/energy/images/CMM/CMM_CE/12._Krause_Skiba_Jura.pdf

[9] E. Krause, B. Jura, J. Skiba, Mining speed control in the coal panel with high coal output concentration. Kontrola prędkości urabiania w ścianach o wysokiej koncentracji wydobycia. Spotkanie Grupy Roboczej Ekspertów ds. metanu z kopalń Europejskiej Komisji Gospodarczej ONZ. Genewa 7-8.11.2019 r.

[10] J. Qin, Q. Qingdong, H. Guo, CFD simulations for longwall gas drainage design optimization. International Journal of Mining Science and Technology **27** (5), 777-782 (2017). DOI: https://doi.org/10.1016/j.ijmst.2017.07.012

[11] E. Krause, Ocena i zwalczanie zagrożenia metanowego w kopalniach węgla kamiennego. Prace Naukowe GIG nr 878. Katowice 2009.

[12] K.M. Tanguturi, R.S. Balusu, Computational fluid dynamics simulations for investigation of parameters affecting goaf gas distribution. Journal of Mining and Environment **9**, 3, 547-557 (2018). DOI: https://doi.org/10.22044/jme.2018.5960.1410

[13] G. Xu, K.D. Luxbacher, S. Ragab, J. Xu, X. Ding, Computational fluid dynamics applied to mining engineering: a review. International Journal of Mining, Reclamation and Environment **31** (4), 251-275 (2017).

[14] Z. Wang, T. Ren, L. Ma, J. Zhang, Investigations of ventilation airflow characteristics on a longwall face – a computational approach. Energies **11**, 1564 (2018). DOI: https://doi.org/10.3390/en11061564

[15] Z. Wang, T. Ren, Y. Cheng, Numerical investigations of methane flow characteristics on a longwall face Part I: Methane emission and base model results, Journal of Natural Gas Science and Engineering **43**, 242-253 (2017).

[16] Z. Wang, T. Ren, Y. Cheng, Numerical investigations of methane flow characteristics on a longwall face Part II: Parametric studies. Journal of Natural Gas Science and Engineering **43**, 242-253 (2017).

[17] SolidWorks Flow Simulation 2012 Technical Reference. https://d2t1xqejof9utc.cloudfront.net/files/18565/SW_CFD_technical_reference.pdf?1361897013